Leg muscles that mediate stability: mechanics and control of two distal extensor muscles during obstacle negotiation in the guinea fowl

Leg muscles that mediate stability: Mechanics and control of two distal extensor muscles during obstacle negotiation in the guinea fowl.

Short title:
Neuromuscular control of running on an obstacle treadmill

Authors: [1]Monica A Daley and [2]Andrew A Biewener

[1]**Author for correspondence**:
Structure and Motion Lab, Royal Veterinary College, University of London, Hawskhead Lane, Hatfield, Hertfordshire, AL97TA, UK. Email: mdaley@rvc.ac.uk

[2] Concord Field Station, Harvard University, 100 Old Causeway Rd, Bedford MA 01730 USA

Abbreviation list:

LG	lateral gastrocnemius muscle
DF	digital flexor muscle head to the lateral toe (digital flexor IV)
TD	toe down (begin stance)
TO	toe off (end stance)
MS	mid-swing point in leg kinematics
H	hip height (usually relative to hip height at TD in level terrain $H_{TD,C}$)
L_{leg}	Effective leg length
LA	Leg angle
EMG	electromyography
F_{pk}	peak muscle-tendon force
T_{rise}	time period from TD to F_{pk}
T_{fall}	time period of force decay from F_{pk} to the initial value
T_{50}	time point of 50% peak force
L_{T50}, V_{T50}	fascicle fractional length (L) and velocity (V) at T_{50}
L_{Fpk}, V_{Fpk}	L and V at F_{pk}
V_{TD_T50}	mean V from TD to T_{50}
V_{T50_pk}	mean V from T_{50} to F_{pk}
Phase	phase between F_{pk} and maximum fascicle length (Phase = $(T_{Fpk}-T_{Lpk})/T_{stride}$)
J_{sw}	force impulse during swing
J_{tot}	force impulse over the stride
W_{sw}	work done during swing
W_{net}	net work over the stride
E_{sw}	swing EMG intensity
E_{tot}	total EMG intensity

Abstract

Here we used an obstacle treadmill experiment to investigate the neuromuscular control of locomotion in uneven terrain. We measured *in vivo* function of two distal muscles of the guinea fowl, lateral gastrocnemius (LG) and digital flexor-IV (DF), during level running, and two uneven terrains, with 5 cm and 7cm obstacles. Uneven terrain required 1 step onto an obstacle every 4-5 strides. We compared both perturbed and unperturbed strides in uneven terrain to level terrain. When the bird stepped onto an obstacle, the leg became crouched, both muscles acted at longer lengths and produced higher work, and body height increased. Muscle activation increased on obstacle strides in the LG, but not the DF, suggesting a greater reflex contribution to LG. In unperturbed strides in uneven terrain, swing pre-activation of DF increased by 5% compared to level terrain, suggesting feed-forward tuning of leg impedance. Across conditions, the neuoromechanical factors in work output differed between the two muscles, likely due to differences in muscle-tendon architecture. LG work depended primarily on fascicle length, whereas DF work depended on both length and velocity during loading. Distal muscles appear to play a critical role in stability by rapidly sensing and responding to altered leg-ground interaction.

Introduction:

The muscles of animal legs must function to allow versatile and stable movement through a wide range of terrain conditions. Yet, little is known about the interplay of mechanics, muscle dynamics and neural control in the context of unsteady tasks such as maneuvering and stabilization (Biewener and Daley, 2007). Animal movement requires a complex integration of central, peripheral and physical control mechanisms (Pearson et al., 1998, Koditschek et al., 2004, Nishikawa et al., 2007). Due to the complexity of the neuromuscular system, multiple possible combinations of muscle activity and sensory feedback can achieve any given target task (Bernstein, 1967, Misiaszek and Pearson, 2002, Ting et al., 2009). However, different solutions for achieving a task may result in different characteristics such as stability, required total muscle activity and fatigue rate (e.g., Bunderson et al., 2008, Ting et al., 2009). Animals likely select among motor control strategies in a context-dependent manner based on numerous criteria (Chiel et al., 2009).

The aim of this study is to investigate the neuromuscular control strategies used by animals to maintain stability in uneven terrain. We are interested in both the immediate response to a perturbation, involving stride-to-stride adjustments, as well as shifts in the motor control strategy depending on terrain environment. In terrain known to be uneven or unpredictable, animals might select a different neuromuscular control strategy than in uniform terrain. For example, when cats are exposed to repeated perturbations to the paw during swing, they exhibit long-term adjustments, 'high-stepping' to avoid stumbling (McVea and Pearson, 2007). Such a strategy has clear advantages in uneven terrain, but might increase energy cost. We expect animals to adjust motor control on both short and longer timescales to achieve robustly stable and economic movement through varying environmental conditions.

An important focus of our investigation is to explore the relationship between muscle-tendon architecture and neuromuscular control. Most *in vivo* studies of muscle function during locomotion have focused on steady locomotion over level ground or a constant slope. To understand the morphological and biomechanical factors that influence neural control, it is critical to investigate muscle dynamics over a broader range of animal behavior. Muscles that play similar roles in steady movement might play distinct roles during non-steady tasks. Here we examine this issue by measuring the *in vivo* force-length-activation dynamics of two distal hindlimb extensors in the guinea fowl: the lateral gastrocnemius (LG) and the digital flexor-IV (DF). These two muscles both have pinnate, short fibered architecture with a relatively long free

tendon. The LG and DF function similarly during steady level locomotion to provide economic weight support during stance and facilitate tendon elastic energy cycling (Roberts et al., 1997, Daley and Biewener, 2003, Gabaldon et al., 2004).

Nonetheless, there are important architectural differences between the LG and DF. The LG acts across the knee and ankle, and has a relatively stiff tendon, whereas the DF crosses the knee, ankle and all distal joints, and has an exceptionally long tendon. The ratio of tendon length to muscle fascicle length is 10.8 for the DF, whereas it is 5.7 for the LG (Daley and Biewener, 2003). The extreme architecture of DF may enhance force control over position control and facilitate economy, but limit its ability to actively control joint position and do external work against the environment (Ker et al., 1988, Alexander, 2002). *In vivo* studies suggest that the DF contributes more than LG to elastic energy cycling in steady running, but does not contribute to work for incline running (Daley and Biewener, 2003). In contrast, the LG contributes moderately to elastic energy cycling, and also contributes to work on an incline (Roberts et al., 1997, Daley and Biewener, 2003, Gabaldon et al., 2004).

Although muscle architecture influences the context in which a muscle does work, its mass determines total work capacity. Short fibered, pinnate distal muscles do have a substantial mass and work capacity in most animals (e.g., Biewener, 1998, Smith et al., 2006). The gastrocnemius and digital flexors of the guinea fowl make up approximately 30% of the hindlimb muscle mass (Daley and Biewener, 2003). We do not yet understand the circumstances in which the distal muscles produce and absorb substantial energy, because muscle force-length dynamics have been measured for relatively few tasks (Biewener and Daley, 2007). Distal muscles may contribute to work during non-steady tasks such as acceleration, jumping, maneuvering and stabilization. Recent work suggests that distal muscles may absorb or produce energy to help stabilize the leg in the face of sudden terrain perturbations (Daley et al., 2007, Daley et al., 2009).

Based on these observations, we hypothesized that the specialized architecture of distal leg muscles reflects a proximo-distal gradient in joint neuromechanical function (Daley et al., 2007, Daley et al., 2009). We suggested that the muscles at proximal joints control leg cycling and contribute the majority of work for tasks such as steady incline running and jumping, whereas distal muscles rapidly adjust force and work during non-steady tasks such as maneuvering, maintaining stability and avoiding injury in uneven terrain. A recent study of *in vivo* dynamics of the LG during running over an unexpected drop in terrain drop supports this idea (Daley et al.,

2009). The LG exhibits rapid changes in work output depending on the posture of the leg when it contacts the ground. This results in a context-dependent stabilizing response to unexpected terrain perturbations.

Here we investigate neuromuscular control of the LG and DF during locomotion over uneven terrain with obstacles repeating every 4-5 strides. The bird must take a single step onto each obstacle before returning to the original ground level. To evaluate the changes in neuromuscular control strategies among terrain conditions, we ask the following four questions:

- How do muscle force-length-activation dynamics during perturbed strides (on obstacle) compare to level terrain?
- How do unperturbed strides in uneven terrain (between obstacles) compare to level terrain?
- Do the LG and DF respond similarly in work output in uneven terrain?
- Do similar neuromechanical factors underlie changes in work of both muscles?

Both unperturbed and perturbed strides in uneven terrain may differ from uniform terrain, due to context-dependent adjustment of motor control. Additionally, the architectural differences between LG and DF may lead to differing responses to perturbations. We expect the DF to be especially sensitive to terrain variation due to its extreme architecture and action at more distal joints. This may result in larger intrinsic mechanical effects on contractile performance, as compared to the LG.

Methods:

Animals and training:

We obtained six adult guinea fowl (*Numida meleagris*), 1.77±0.26 kg body mass (mean±s.e.m., N=6) from a local breeder near Bedford, Massachusetts. Animals were trained to run on a level motorized treadmill (Woodway, Waukesha, WI) at speeds of 1.7-2.0 ms^{-1}. Training sessions were 20-30 minutes in duration, with breaks for 1-3 minutes as needed. Animals were trained 3-4 days per week for 3 weeks. Experiments were undertaken at the Concord Field Station of Harvard University. All procedures were approved by the Harvard Institutional Animal Care and Use Committee.

Surgical procedures

We followed similar surgical procedures as described previously (Daley and Biewener, 2003). Transducers were implanted into the lateral head of the gastrocnemius (LG) and the digital flexor

to the lateral toe (DF). The birds were anesthetised using isoflurane delivered through a mask. The surgical field was plucked of feathers and sterilised with antiseptic solution (Prepodyne, West Argo, Kansas City, MO). Transducers were connected to a micro-connector placed on the bird's back (GM-6, Microtech Inc, Boothwyn, PA USA). We passed the transducer leads subcutaneously from a 1–2 cm incision over the synsacrum to a second 4–5 cm incision over the lateral right shank. E-type tendon buckle force transducers were implanted on the Achilles tendon and DF tendon. Sonomicrometry crystals (0.7mm for DF, 1.0 mm for LG; Sonometrics Inc., London, Canada) were implanted along the fascicle axis in the middle 1/3rd of each muscle. Crystals were placed in small openings created using fine forceps, approximately 3–4 mm deep and 10 mm apart. We verified signal quality using an oscilloscope, and then secured them by closing the overlying connective tissue with 5-0 silk suture.

Next to each sonomicrometry crystal pair, we implanted fine-wire, twisted, silver bipolar EMG hook electrodes with 0.1 mm diameter, 0.5-1.0 mm bared tips, 5-8 mm spacing (California Fine Wire, Inc., Grover Beach, USA). EMG electrodes were placed using a 23 gauge hypodermic needle and secured to the muscle's fascia using 5-0 silk suture. Skin incisions were closed using 3-0 silk. The birds could walk within 2 hours and ran the following day without lameness. The birds were given analgesia every 12 hours and antibiotics every 24 hrs. Experimental recordings took place over the next 1-3 days. After the experiments, the guinea fowl were killed by an intravenous injection of sodium pentobarbital (100 mg kg^{-1}) under deep isoflurane anaesthesia (4%, mask delivery).

Post mortem, we dissected each muscle free from the surrounding tissues to make morphological measurements and confirm placement of transducers. Crystal alignment relative to the fascicle axis (α) was within ± 3°. Finally, the tendon force buckles were calibrated *in situ* (Daley and Biewener, 2003).

Transducer Recording

The microconnector on the bird's back was connected, via a lightweight shielded cable (Cooner Wire, Chatsworth, USA), to a sonomicrometry amplifier (120.2 , Triton Technology Inc., San Diego, USA), a strain gauge bridge amplifier (2120, Vishay Micromeasurements, Raleigh, USA), and EMG amplifiers (P-511, Grass, West Warwick, USA). EMG signals were amplified 1000X and filtered (10 Hz – 10 kHz bandpass) before digital sampling. Signals were sampled by an A/D converter (Axon Instruments, Union City, USA) at 5 kHz.

Kinematics

Digital high-speed video was recorded in lateral view at 250 Hz (PhotronFastcam-X 1280 PCI; Photron USA Inc., San Diego, CA, USA). Kinematic points were marked on the synsacrum, hip, middle toe and lateral toe, and tracked using custom software in MATLAB (v7, Mathworks, Inc.; Natick, MA, USA). We tracked the following kinematic events 1) midswing (MS), the time at which the swing-leg toe crossed the midline of the stance leg; 2) toe down (TD) and 3) toe off (TO). Successive MS events were used to cut the muscle data into strides. For a subset of data, we manually digitised the marker positions at the kinematic events. We calculated effective leg length (L_{leg}), leg angle (LA), hip height (H) (Fig. 1a), stride period and stance period.

Experimental protocol

The guinea fowl ran at 1.7 m/s in three conditions 1) level terrain, 2) terrain with repeated 5 cm high obstacles and 3) terrain with repeated 7 cm high obstacles. In uneven terrain, the bird encountered an obstacle every 4-5 strides. We constructed the obstacles using Styrofoam covered with cardboard and black neoprene, to create a light, stiff surface that matched treadmill belt. The treadmill belt was composed of rubber-coated steel slats (0.56 m x 0.07 m) with clearance around the entire surface for obstacles. The effective running surface measured 0.56 m x 1.73 m. We matched the length and width of individual obstacles to the belt slats, and attached them with industrial strength Velcro®. Seven obstacles were placed on sequential slats to form a total obstacle surface that was 0.49 m long, approximately one stride length.

Data processing

We filtered the EMG signals using a sixth order, zero-lag high-pass Butterworth filter (70 Hz cutoff), then calculated the intensity over time using wavelet analysis as described previously (Daley et al., 2009). Within individuals, EMG intensity was normalized based on the mean total intensity per stride in level trials. We calculated fractional fascicle length from the sonomicrometry data, following methods described by others (Gillis and Biewener, 2002), using length during quiet standing as the reference length (L_o). Fascicle length was differentiated to obtain fascicle velocity (V, in lengths per second, Ls^{-1}). To calculate muscle power, velocity (converted to ms^{-1}) was multiplied by tendon force (in Newtons). Muscle power was integrated over time for each stride to calculate work (in Joules, and divided by muscle mass to obtain mass specific values, Jkg^{-1}). We then measured variables at a number of time points to evaluate muscle force, length and activation dynamics, see the abbreviation list for a description.

Statistics

For each trial we analyzed a 10-12 second sequence in which the bird maintained a constant speed, resulting in approximately 30 strides per trial. Stride cycles were put into the following categories: control (C) for level running, and in uneven terrain the stride prior to (s -1), the stride on (s 0), the first stride following (s 1), and the second to third strides following (s 2) an obstacle. We grouped strides 2-3 together because the number of strides between obstacles varied.

All statistics were calculated using the statistics toolbox in MATLAB (Mathworks, Inc.; Natick, MA, USA). To test for differences in muscle and kinematic variables, we used mixed model ANOVA with stride category as a fixed factor and individual as a random factor. We used posthoc t-tests with Bonferroni correction to compare pairs of stride categories.

We used multiple linear regression analysis to evaluate the contributions of fascicle length, phase and activation factors on total force impulse (J_{tot}) and net work produced (W_{net}) by each muscle. We included L_{T50}, V_{T50}, L_{Fpk}, V_{Fpk}, Phase, E_{sw} and E_{tot} as factors in the model (see abbreviation list), with backward stepping to minimize multicolinearity and find the minimal model that best fit the data.

Results:

Changes in kinematics and leg posture during perturbed strides in uneven terrain

When guinea fowl negotiated an obstacle, the leg contacted the obstacle during late swing, initiating an early transition to stance compared to level terrain (Figs. 1 and 2). The birds exhibited a more 'crouched' leg posture on the obstacle, with a shallower leg angle and shorter hip height (Fig. 1b, Tab. 1). Hip height increased during stance by 3.2 cm on both 5 and 7cm obstacles, suggesting net positive work on the body (Fig. 1b; Tab. 1).

Muscle force-length-activation dynamics during perturbed strides in uneven terrain

Significant changes occurred in muscle force-length dynamics during obstacle strides in relation to altered leg loading and posture. As the foot contacted the obstacle, fascicle length of both LG and DF immediately diverged from level means (Figs. 2 and 3), shifting towards longer lengths. Force development began early in both muscles (Fig. 3) and the rise time to peak force (T_{rise}) took longer (Tab. 2). LG peak force (F_{pk}) increased by 32 and 39% in 5 and 7cm terrain, respectively; in contrast, DF F_{pk} decreased by 20% and 26% (Tab. 2). EMG intensity (E_{tot}) of LG increased by

over 80% in obstacle strides in 5cm and 7cm terrain; in contrast, there was no significant change in E_{tot} of the DF (Fig. 5, Tab. 2).

The average shifts in length and velocity on obstacle strides were similar for the two muscles ('s 0', Fig. 4). Fascicle length remained longer throughout force development on obstacles (Fig. 3). Velocity shifted towards increased stretch during the initial loading phase from TD to T_{50} (V_{TD_T50}), and towards greater shortening (or less stretch) from T_{50} to F_{pk} (V_{T50_Fpk}) ('s 0', Fig. 4).

Overall, force-length dynamics in obstacle strides led to significantly greater work output compared with level control (Fig. 5, Tab. 2). LG work (W_{net}) on 's 0' increased by 5.26 and 6.05 Jkg^{-1} for 5 and 7 cm terrain, respectively. The DF also showed increased W_{net}, averaging 9.16 and 13.79 Jkg^{-1} in 5 and 7 cm terrain; however the difference was significant only for 7 cm terrain, due to high variation in DF work output (Fig. 5, Tab. 2).

Muscle force-length-activation dynamics during 'unperturbed' strides in uneven terrain

The largest shifts in force, length and activation occurred in obstacle strides (s 0); however, there were also a number of significant shifts across non-obstacle strides. In the stride immediately following the obstacle (s 1), force-length dynamics were similar to level terrain (Tab. 2). A greater number of differences occurred in strides immediately preceding the obstacle (s -1) and during unperturbed strides between obstacles (s 2). Across non-obstacle strides, swing phase activation (E_{sw}) increased by about 5%, although this difference was significant only for DF (Tab. 2). The DF operated at 5% shorter lengths in 5 cm terrain (Tab. 2). LG velocity shifted towards stretch, by about 1.5 Ls^{-1} from TD to T_{50}, and 0.7 Ls^{-1} from T_{50} to F_{pk} (Fig. 4). LG W_{net} decreased by 1 Jkg^{-1} in 5cm terrain (Fig. 5). The total force impulse in unperturbed strides in uneven terrain did not differ significantly from level control (Tab. 2).

Contractile properties underlying the changes in muscle work in uneven terrain

The force-length dynamics of the LG and DF varied substantially in uneven terrain, depending on how the leg interacted with the ground. Muscle length and force development rapidly deviated from level values as soon as the foot contacted the obstacle (Fig. 2 and 3). The DF exhibited more time-varying force-length dynamics within a stride, greater stride-to stride variation (Fig. 3), and a greater range of mass-specific work output (Fig. 6), compared to the LG.

Multiple regression analysis suggests that a number of neuromechanical factors contributed to variation in LG and DF mechanical output. The largest factor in the regression model for total force impulse (J_{tot}) was length at 50% peak force (L_{T50}), for both LG and DF. L_{T50} explained 60% of the variation in J_{tot} for the LG, and 30% for the DF (Tab. 3). For the LG, V_{T50} and E_{tot} also contributed to the variation in J_{tot}, explaining 7% and 9% of the variance, respectively. For the DF, these factors did not contribute to the model for J_{tot}. Phase (between force and length) and swing E_{sw} were significant factors for the DF, but explained only 1 and 5% of the variance, respectively. The results suggest that 67% of LG variance and 31% of DF variance in J_{tot} could be explained by intrinsic mechanical factors relating to length and velocity. However, the total variance explained (R^2) by the model for J_{tot} was lower for the DF ($R^2 = 0.76$ for LG and 0.36 for DF), suggesting that a linear model may not be adequate for this muscle.

The neuromechanical factors in W_{net} differed more substantially between muscles. L_{T50} was the largest single factor in LG W_{net}, explaining 64% of variance, whereas velocity at peak force (V_{Fpk}) was the largest factor in DF W_{net}, explaining 31% of variance. Additional factors in LG work were V_{Fpk}, E_{sw} and E_{tot}, explaining 4, 1 and 7% of the variance, respectively. For DF work, L_{T50} and Phase (between force and length) were additional significant factors, each explaining 16% of the variance. Activation factors (E_{sw}, E_{tot}) contributed significantly to variation in W_{net} of the LG, but not the DF.

Relationship between leg posture and force-length dynamics across terrain conditions

The fascicle length of both muscles inversely correlated with leg posture (Fig 7a). More crouched postures at TD led to greater extremes in fascicle length during force development. There was also an inverse relationship between leg posture and the change in hip height during stance (ΔH; Fig. 7b). Changes in hip height provide an estimate of the potential energy change of the body, so the positive ΔH associated with crouched leg posture suggests net positive work on the body. The significant positive correlation between L_{T50} and W_{net}, observed for both muscles (Tab. 3, Fig. 6), suggests that the LG and DF both contribute to an increase in potential energy of the body when the leg contacts the ground in a crouched posture.

Discussion:

Recent studies investigating leg and muscle mechanics in response to an unexpected terrain drop suggest that distal leg muscles play an important role in stability and injury prevention during running over uneven terrain (Daley et al., 2007, Daley et al., 2009). The response depends on the

interplay of leg posture, leg loading and neuromuscular control (Daley et al., 2009). However, the previous studies focused on a single unexpected drop perturbation that may not reflect natural terrain conditions. Here, we investigated context-dependent changes in neuromuscular control in uneven terrain. We measured *in vivo* muscle function of two distal muscles, lateral gastrocnemius (LG) and digital flexor-IV (DF), during running over terrain with obstacles every 4-5 strides. This terrain was not particularly challenging— the birds maintained average position on the treadmill belt and recovered from each obstacle within one stride following the perturbation.

How do neuromuscular dynamics during perturbed strides (on obstacle) compare to level terrain?

The bird's dynamic response to the perturbed obstacle stride (s 0) in uneven terrain is similar to that observed during an unexpected drop perturbation (Daley et al., 2009). Leg posture was more crouched and stance duration longer in obstacle strides, but stride duration remained similar (Tab. 1). Muscle length was similar to level running until the toe contacted the obstacle (Fig. 3). The kinematic differences may have resulted from the intrinsic mechanical interaction of the swing leg with the obstacle, resulting in an early transition from swing to stance. Drop perturbations result in similar but inverse dynamics— delayed ground contact leads to a more extended leg posture and shorter stance duration (Daley and Biewener, 2006).

In both obstacle and drop perturbation conditions, there is a strong relationship between the work produced by LG and leg posture at the time of ground contact (Fig. 8) (Daley et al., 2009). The drop perturbation experimented elicited greater extremes in LG work and leg posture. This is likely due to the larger size of the perturbation used: 8.5 cm (Daley et al., 2006), compared to 5 and 7 cm in the current study. However, additional factors may contribute, such as variation in feed-forward control and reflex modulation across conditions, because LG work in the unexpected drop diverges more from the fit to both data sets (Fig. 8). Nonetheless, the trends are remarkably similar. Similar to the LG, the DF muscle exhibits rapid changes in force-length dynamics and work output during obstacle perturbed strides. The average change in work of the DF was higher than that of the LG (Fig. 5), but DF showed greater-stride to-stride variability. Neural factors appear to play a greater role in the response of the LG during perturbed obstacle strides, as compared to the DF. Total EMG intensity of the LG increased by over 80% on the obstacle stride (s 0), but DF activity was not significantly different from level running. In the unexpected drop experiment, there was no significant change in LG EMG activity within the perturbed stride (Daley et al., 2009). This suggests either that neuromuscular control of LG is

adjusted in anticipation of the obstacle in uneven terrain, or that the reflex response to a sudden increase in load differs from the response to a sudden decrease in load. The transmission delay for the stretch reflex of the gastrocnemius is approximately 6 ms, which is less than 5% of stance duration (Nishikawa et al., 2007), so monosynaptic (Ia) stretch reflexes could explain the increase in LG muscle activity. Additionally, heterogenic length feedback between agonist muscles acts in approximately the same time scale (Nichols, 1999). Feedback from the DF as the toes contact the obstacle could excite LG activity through heterogenic pathways. Head pitch is another factor that could facilitate increased LG muscle activity in the obstacle stride. In cats, pitching the head downward elicits increased muscle activity analogous to uphill walking (Gottschall and Nichols, 2007). If guinea fowl look downward in anticipation of obstacles, this could elicit increased LG activity similar to that observed on steady inclines (Roberts et al., 1997, Carlson-Kuhta et al., 1998).

How do neuromuscular dynamics during unperturbed strides (between obstacles) compare to level terrain?

The kinematics in unperturbed strides remained similar to level terrain, suggesting that the overall target movement pattern is not adjusted in uneven terrain. There were no significant differences in kinematic variables in the unperturbed strides (Tab. 1). Interestingly, the final leg angle before toe off (LA_{TO}) did not change significantly in any stride category (Tab. 1), suggesting consistent control of the stance-swing transition. Cat studies suggest that the stance-swing and stance-swing transitions are controlled through a combination of two sensory signals: loading of ankle extensors, and position feedback from hip extensors (Duysens and Pearson, 1980, Hiebert et al., 1996). The consistency of LA_{TO} across conditions may result from physical unloading of the leg beyond a particular angle, providing robust control of stance-swing transition across varied terrain conditions.

Although the overall movement pattern was not adjusted in the unperturbed strides in uneven terrain, muscle dynamics suggest context-depending tuning of neuromuscular control. Swing phase activation increased by 5% across unperturbed strides, which may facilitate a rapid response when the leg contacts an obstacle. DF operated at 5% shorter length in uneven terrain, and LG shifted towards stretch during force development (Tab. 2). These findings suggest that animals might tune force-length dynamics through small shifts in the timing of muscle activation. This is consistent with other recent studies that suggest context-depending tuning of control; even when similar overall gait and speed are maintained. For example, humans and other animals

adjust leg compliance through posture and co-activation (Moritz and Farley, 2004), foot placement to avoid obstacles (Marigold and Patla, 2007), and swing leg kinematics to avoid stumbling (McVea and Pearson, 2007). Yet, we still have a limited understanding of how animals select among control strategies while moving through complex terrain. This is because most of our knowledge of locomotion is based on controlled laboratory conditions, usually on steady, level locomotion on treadmills or uniform runways, or in 'reduced' preparations where much of the central nervous control has been removed or minimized (Pearson et al., 2006, Biewener and Daley, 2007). Further studies are required that include both naturalistic terrains and neuromechanical simulations. Nonetheless, the results here suggest that animals use similar target movements across terrain conditions, with feed-forward adjustments and reflex feedback acting to tune leg impedance around the same global strategy.

Neuromechanical factors contributing to the changes in muscle dynamics of LG and DF

The LG and DF differ in muscle-tendon morphology: although both have pinnate, short fibered architecture, the DF has an exceptionally long tendon that crosses all distal joints. We expected the DF to be more sensitive to terrain perturbations due to its extreme architecture. Although the average fascicle length and velocity changes were similar for the two muscles (Fig. 4), the DF produced a greater range of work over the conditions measured (Fig. 6). This is consistent with results on steady level and incline running (Daley and Biewener, 2003), suggesting that the stretch-shorten cycle of the DF results in greater sensitivity in work output to variation in length, velocity and phase. The DF has a weaker relationship between fascicle length and work than the LG, but greater sensitivity to velocity (Tab. 3). The LG acts as a length-dependent actuator, generating positive work when the leg begins stance in a more crouched posture. In contrast, the DF acts as both a length- and velocity- dependent actuator. Work done by the DF depends on both leg posture and how rapidly the leg is loaded.

Although there are a number of adjustments to neural control in uneven terrain, it appears that intrinsic mechanical factors play a large part in the response of both LG and DF. The delay between activation and force development is approximately 30 ms in level running (Daley et al., 2009), suggesting that intrinsic mechanical factors lead to the initial rapid increase in force upon obstacle contact. Length and velocity were the largest factors in total force impulse and work of both muscles (Tab. 3). Furthermore, DF exhibited an increase in mean work on obstacle steps, despite similar total EMG intensity (Fig. 5). Changes in fascicle length can immediately alter muscle contraction due to force-length and force-velocity properties of muscle (Hill, 1938,

Gordon et al., 1966). History-dependent factors, such as stretch force enhancement, might also contribute (Edman et al., 1978). The small shifts in swing pre-activation may tune these intrinsic mechanics effects by adjusting muscle length and velocity during the loading phase of stance.

A tradeoff in limb design for economy versus stability?

We propose that the diversity in distal leg muscle architecture among animals reflects tradeoffs among economy *versus* stability, injury avoidance and agility. Specialist hoppers and runners, such as wallabies and horses, have distal architecture that facilitates economy through short, pinnate fiber arrangement and long tendons (Biewener and Baudinette, 1995, Biewener et al., 1998). However, wallaby distal muscles do not increase work output on an incline (Biewener et al., 2004), and horse digital flexors may be limited to a high-frequency damping function (Wilson et al., 2001). Furthermore, horse distal tendons are prone to injury and heat damage (Wilson and Goodship, 1994, Williams et al., 2001). In contrast, the ankle extensors of generalists such as ducks, guinea fowl and turkeys, store relatively less elastic energy, but likely have higher safety factors and can control work against the environment for other tasks, such as swimming (ducks) and incline running (guinea fowl, turkeys) (Roberts et al., 1997, Biewener and Corning, 2001, Daley and Biewener, 2003, Gabaldon et al., 2004). This and other recent studies suggest that distal extensor muscles also play a critical role in stability by rapidly adjusting work output in response to terrain perturbations (Daley and Biewener, 2006, Daley et al., 2007, Daley et al., 2009). Consequently, distal muscles might have greater mass and work capacity in animals that regularly negotiate uneven terrain. The guinea fowl is a capable runner, but also relatively small. Small animals may live in inherently 'rough' environments, frequently encountering large terrain changes relative to leg length. Thus, guinea fowl distal hindlimb morphology may reflect optimization toward robust stability in uneven terrain.

Acknowledgements:
We thank colleagues at the Concord Field Station of Harvard University for assistance and feedback, including Craig McGowan, Jim Usherwood, Polly McGuigan, Russ Main, Ed Yoo, Chris Richards and Pedro Ramirez. Supported by an HHMI Predoctoral Fellowship and an NSF Bioinformatics Postdoctoral Fellowship to M.A.D. (DBI-0630664), and an NIH grant (AR047679) to A.A.B.

Figure Legends:

Figure 1. A) Still frames of the guinea fowl at the point of toe down (TD) during level running (left) and negotiation of a 5 cm obstacle (right), illustrating measurement of relative leg length (L_{leg}) and hip height (H). In **B**) the mean+- S.E.M values for hip height at toe down (H_{TD}), hip height at toe off (H_{TO}), and the change in hip height over stance (ΔH) are shown for three stride categories: just before the obstacle (s -1), on the obstacle (s 0) and in the mid-flat section between obstacles (s 2). Values are shown as the fractional difference from the level terrain mean (horizontal line), with asterisks indicating statistical significance.

Figure 2. Muscle recordings from the lateral gastrocnemius (LG, top) and digital flexor-IV (DF, bottom) during level running (gray dashed lines) and obstacle running (blue and green solid lines for LG and DF, respectively). Markers on the force traces indicate kinematic event timing: midswing (MS, rectangle), toe down (TD, down triangle), toe off (TO, up triangle). The traces for the two conditions are aligned in time at MS before the third stride in the trace (dashed vertical line). In the obstacle example, the solid vertical line indicates the time of first toe contact with an obstacle.

Figure 3. Fascicle length, muscle force (N) and EMG intensity (mV), for Ind. 5 over a stride for LG (left) and DF (right). Gray lines indicate the mean±s.e.m. for level running. Blue and green lines (for LG and DF, respectively) show three 5 cm obstacle strides to illustrate stride-to-stride variation. EMG traces shown here are rectified and box filtered using a 20-point (4 ms) box filter.

Figure 4. Fascicle length (left) and velocity (right) values across stride categories (mean±s.e.m.), relative to the level terrain means (LG: blue 'o', DF: green 'x'; 5cm terrain- smaller symbols, 7cm terrain, larger symbols). Grey box indicates the obstacle stride (s o). Fascicle length is shown at the time of 50% peak force (L_{T50}), and peak force (L_{Fpk}). Velocity is shown for the initial loading phase from TD to 50% peak force (V_{TD_T50}) and from 50% to peak force (V_{T50_Fpk}). Positive velocity indicates a shift toward muscle stretch (or reduced shortening). On obstacle steps, the muscles operated at longer lengths, and underwent greater stretch early in loading, but greater shortening (or less stretch) from T_{50} to peak force (see Table 2 for ANOVA).

Figure 5. Changes in force impulse, work and EMG intensity for the LG and DF during swing phase (left) and the full stride (right) across stride categories (mean±s.e.m.), relative to the level terrain mean. Symbols as in Figure 4 (see Table 2 for ANOVA).

Figure 6. Comparison of operating ranges for LG (blue 'o') and DF (green 'x') in work, fascicle length at 50% peak force (L_{T50}, **a**) and velocity at peak force (V_{Fpk}, **b**). Both L_{T50} and V_{Fpk} significantly influenced work according to the regression analysis (Table 3).

Figure 7. A) Both LG (blue 'o') and DF (green 'x') exhibited an inverse correlation between fascicle length at 50% force (L_{T50}) and hip height at toe down (H_{TD}). **B)** Change in hip height during stance (ΔH) inversely correlated with H_{TD}.

Figure 8. Work of the LG in relation to H_{TD}, for obstacle terrain (darker symbols) and an unexpected drop perturbation (lighter symbols, (Daley et al., 2009)). The relationship is similar in both conditions, although the previous study elicited greater extremes in both leg posture and LG muscle work due to the larger size of the terrain change. Across both conditions, LG work inversely correlates with initial leg posture (R^2 = 0.72). The silhouettes schematically illustrate leg postures for positive and negative terrain changes (modified from Daley et al. 2009).

References:

Alexander, R. M. 2002. Tendon elasticity and muscle function. *Comparative Biochemistry and Physiology a-Molecular and Integrative Physiology,* 133**,** 1001-1011.

Bernstein, N. 1967. *The Co-ordination and Regulation of Movements*, Oxford, UK: Pergamo.

Biewener, A. A. 1998. Muscle function in vivo: A comparison of muscles use for elastic energy savings versus muscles used to generate mechanical power. *Am Zool,* 38**,** 703-717.

Biewener, A. A. & Baudinette, R. V. 1995. In vivo muscle force and elastic energy storage during steady-speed hopping of tammar wallabies (Macropus eugenii). *J Exp Biol,* 198**,** 1829-1841.

Biewener, A. A. & Corning, W. R. 2001. Dynamics of mallard (Anas platyrhynchos) gastrocnemius function during swimming versus terrestrial locomotion. *J Exp Biol,* 204**,** 1745-1756.

Biewener, A. A. & Daley, M. A. 2007. Unsteady locomotion: integrating muscle function with whole body dynamics and neuromuscular control. *J Exp Biol,* 210**,** 2949-2960.

Biewener, A. A., Konieczynski, D. D. & Baudinette, R. V. 1998. In vivo muscle force-length behavior during steady speed hopping in tammar wallabies. *J Exp Biol,* 201**,** 1681-1694.

Biewener, A. A., Mcgowan, C., Card, G. M. & Baudinette, R. V. 2004. Dynamics of leg muscle function in tammar wallabies (M. eugenii) during level versus incline hopping. *J Exp Biol,* 207**,** 211-223.

Bunderson, N. E., Burkholder, T. J. & Ting, L. H. 2008. Reduction of neuromuscular redundancy for postural force generation using an intrinsic stability criterion. *J Biomech,* 41**,** 1537-1544.

Carlson-Kuhta, P., Trank, T. V. & Smith, J. L. 1998. Forms of Forward Quadrupedal Locomotion. II. A Comparison of Posture, Hindlimb Kinematics, and Motor Patterns for Upslope and Level Walking. *J Neurophysiol,* 79**,** 1687-1701.

Chiel, H. J., Ting, L. H., Ekeberg, O. & Hartmann, M. J. Z. 2009. The Brain in Its Body: Motor Control and Sensing in a Biomechanical Context. *J Neurosci,* 29**,** 12807-12814.

Daley, M. A. & Biewener, A. A. 2003. Muscle force-length dynamics during level versus incline locomotion: a comparison of in vivo performance of two guinea fowl ankle extensors. *J Exp Biol,* 206**,** 2941-2958.

Daley, M. A. & Biewener, A. A. 2006. Running over rough terrain reveals limb control for intrinsic stability. *Proc Natl Acad Sci U S A,* 103**,** 15681-15686.

Daley, M. A., Felix, G. & Biewener, A. A. 2007. Running stability is enhanced by a proximo-distal gradient in joint neuromechanical control. *J Exp Biol,* 210**,** 383-394.

Daley, M. A., Usherwood, J. R., Felix, G. & Biewener, A. A. 2006. Running over rough terrain: guinea fowl maintain dynamic stability despite a large unexpected change in substrate height. *J Exp Biol,* 209**,** 171-187.

Daley, M. A., Voloshina, A. & Biewener, A. A. 2009. The role of intrinsic muscle mechanics in the neuromuscular control of stable running in the guinea fowl. *J Physiol,* 587**,** 2693-2707.

Duysens, J. & Pearson, K. G. 1980. Inhibition of flexor burst generation by loading ankle extensor muscles in walking cats. *Brain Res,* 187**,** 321-332.

Edman, K. A. P., Elzinga, G. & Noble, M. I. M. 1978. Enhancement of mechanical performance by stretch during tetanic contractions of vertebrate skeletal muscle fibres. *J Physiol (Lond),* 281.

Gabaldon, A. M., Nelson, F. E. & Roberts, T. J. 2004. Mechanical function of two ankle extensors in wild turkeys: shifts from energy production to energy absorption during incline versus decline running. *J Exp Biol,* 207**,** 2277-2288.

Gillis, G. B. & Biewener, A. A. 2002. Effects of surface grade on proximal hindlimb muscle strain and activation during rat locomotion. *J Appl Physiol,* 93**,** 1731-1743.

Gordon, A. M., Huxley, A. F. & Julian, F. J. 1966. Variation in Isometric Tension with Sarcomere Length in Vertebrate Muscle Fibres. *J Physiol,* 184**,** 170-+.

Gottschall, J. S. & Nichols, T. R. 2007. Head pitch affects muscle activity in the decerebrate cat hindlimb during walking. *Exp Brain Res***,** 131-135.

Hiebert, G. W., Whelan, P. J., Prochazka, A. & Pearson, K. G. 1996. Contribution of hind limb flexor muscle afferents to the timing of phase transitions in the cat step cycle. *J Neurophysiol,* 75**,** 1126-1137.

Hill, A. V. 1938. The heat of shortening and the dynamic constants of muscle. *Proc R Soc Lond B Biol Sci,* 126**,** 136-195.

Ker, R. F., Alexander, R. M. & Bennet, M. B. 1988. Why are mammalian tendons so thick? *J Zool Lond,* 216**,** 309-324.
Koditschek, D. E., Full, R. J. & Buehler, M. 2004. Mechanical aspects of legged locomotion control. *Arthropod Structure and Development,* 33**,** 251-272.
Marigold, D. S. & Patla, A. E. 2007. Gaze fixation patterns for negotiating complex ground terrain. *Neuroscience,* 144**,** 302-313.
Mcvea, D. A. & Pearson, K. G. 2007. Long-lasting, context-dependent modification of stepping in the cat after repeated stumbling-corrective responses. *Journal of Neurophysiology,* 97**,** 659-669.
Misiaszek, J. E. & Pearson, K. G. 2002. Adaptive changes in locomotor activity following botulinum toxin injection in ankle extensor muscles of cats. *J Neurophysiol,* 87**,** 229-239.
Moritz, C. T. & Farley, C. T. 2004. Passive dynamics change leg mechanics for an unexpected surface during human hopping. *J Appl Physiol,* 97**,** 1313-1322.
Nichols, T. R. 1999. Receptor mechanisms underlying heterogenic reflexes among the triceps surae muscles of the cat. *J Neurophysiol,* 81**,** 467-478.
Nishikawa, K., Biewener, A. A., Aerts, P., Ahn, A. N., Chiel, H. J., Daley, M. A., Daniel, T. L., Full, R. J., Hale, M. E., Hedrick, T. L., Lappin, A. K., Nichols, T. R., Quinn, R. D., Satterlie, R. A. & Szymik, B. 2007. Neuromechanics: an integrative approach for understanding motor control. *Integr Comp Biol,* 47**,** 16-54.
Pearson, K., Ekeberg, O. & Buschges, A. 2006. Assessing sensory function in locomotor systems using neuro-mechanical simulations. *Trends Neurosci,* 29**,** 625-631.
Pearson, K. G., Misiaszek, J. E. & Fouad, K. 1998. Enhancement and resetting of locomotor activity by muscle afferents. *In:* KIEHN, O., HARRIS-WARRICK, R. M., JORDAN, L. M., HULTBORN, H. & KUDO, N. (eds.) *Neuronal Mechanisms for Generating Locomotor Activity.*
Roberts, T. J., Marsh, R. L., Weyand, P. G. & Taylor, C. R. 1997. Muscular force in running turkeys: the economy of minimizing work. *Science,* 275**,** 1113-1115.
Smith, N. C., Wilson, A. M., Jespers, K. J. & Payne, R. C. 2006. Muscle architecture and functional anatomy of the pelvic limb of the ostrich (Struthio camelus). *J Anat,* 209**,** 765-779.
Ting, L. H., Van Antwerp, K. W., Scrivens, J. E., Mckay, J. L., Welch, T. D. J., Bingham, J. T. & Deweerth, S. P. 2009. Neuromechanical tuning of nonlinear postural control dynamics. *Chaos: An Interdisciplinary Journal of Nonlinear Science,* 19**,** 026111-12.
Williams, R. B., Harkins, L. S., Hammond, C. J. & Wood, J. L. N. 2001. Racehorse injuries, clinical problems and fatalities recorded on British racecourses from flat racing and National Hunt racing during 1996, 1997 and 1998. *Equine Vet J,* 33**,** 478-486.
Wilson, A. M. & Goodship, A. E. 1994. Exercise-Induced Hyperthermia as a Possible Mechanism for Tendon Degeneration. *J Biomech,* 27**,** 899-&.
Wilson, A. M., Mcguigan, M. P., Su, A. & Van Den Bogert, A. J. 2001. Horses damp the spring in their step. *Nature,* 414**,** 895-899.

Table 1. Kinematic results for mixed-model ANOVA. * Indicates significance of pairwise comparison to level.

Level terrain (Control)		ANOVA results		Uneven terrain, by stride category					
				5cm obstacle terrain			7cm obstacle terrain		
Variable	**mean(SD)**	**F**	**P**	**-1**	**0**	**2**	**-1**	**0**	**2**
$L_{leg,TD}$ (cm)	25.8(0.02)	47.05	<0.001	0.5±0.5	**-2.3±0.7***	1.1±0.2	-0.1±0.3	**-3.4±0.5***	0.0±0.4
H_{TD} (cm)	18.2(0.02)	124.92	<0.001	0.5±0.3	**-3.8±0.2***	0.6±0.1	0.1±0.2	**-4.5±0.3***	0.0±0.3
LA_{TD} (deg)	44.8(1.2)	36.65	<0.001	0.4±0.6	**-7.3±0.9***	-0.8±0.1	0.7±1.3	**-7.4±1.3***	-0.1±1.1
LA_{TO} (deg)	119.9(1.9)	1.08	0.3788	-2.1±1.4	-0.3±2.3	-0.6±0.0	-1.2±1.0	-2.1±2.2	-0.1±0.5
ΔH (cm)	-1.0(0.95)	39.16	<0.001	0.0±0.2	**3.2±0.5***	-0.2±0.1	-0.3±0.3	**3.2±0.4***	0.1±0.1
Stance (ms)	195(47)	7.9	<0.001	-16±9	**35±25***	-30±8	-19±12	14±24	-14±17
Stride (ms)	376(43)	2.26	0.0413	-9±15	21±23	-25±10	-22±16	1±28	-9±21

Table 2. *In vivo* muscle results for mixed-model ANOVA. * Indicates significance of pairwise comparison to level.

A) ANOVA results **B)** Normalised least-squares mean difference from level, by stride category (LSMD ± SEM)

			5cm obstacle terrain				7cm obstacle terrain			
LG	**F**	**P**	**-1**	**0**	**1**	**2**	**-1**	**0**	**1**	**2**
L_{T50} ($L/L_{Fpk,c}$)	179.28	<0.001	**-0.03±0.02***	**0.26±0.06***	0.00±0.02	**-0.03±0.02***	-0.01±0.01	**0.31±0.05***	0.01±0.02	-0.01±0.01
L_{Fpk} ($L/L_{Fpk,c}$)	104.73	<0.001	0.00±0.02	**0.16±0.05***	0.02±0.03	0.00±0.02	0.00±0.01	**0.18±0.03***	0.00±0.02	0.00±0.01
V_{TD_T50} ($V-V_c$, Ls^{-1})	12.57	<0.001	**1.53±0.42***	**3.04±1.39***	**1.60±0.28***	**1.71±0.44***	**1.18±0.19***	**2.45±1.17***	**1.64±0.52***	**1.35±0.29***
V_{T50_Fpk} ($V-V_c$, Ls^{-1})	56.18	<0.001	**0.85±0.33***	**-1.76±0.56***	0.41±0.34	**0.71±0.31***	0.34±0.37	**-2.30±0.49***	-0.20±0.18	0.28±0.25
J_{sw} ($J/J_{pk,c}$)	1.96	0.049	0.01±0.02	0.00±0.03	0.01±0.03	0.01±0.02	0.01±0.02	0.02±0.03	0.01±0.01	0.01±0.01
J_{tot} ($J/J_{pk,c}$)	119.77	<0.001	-0.06±0.04	**0.67±0.19**	-0.04±0.04	-0.06±0.04	-0.01±0.04	**0.81±0.15**	0.01±0.05	-0.02±0.03
F_{pk} ($F/F_{pk,c}$)	50.09	<0.001	**-0.08±0.02***	**0.32±0.13***	-0.03±0.03	**-0.04±0.02***	-0.04±0.02	**0.39±0.12***	0.04±0.03	0.00±0.03
T_{rise} ($T-T_c$, ms)	6.53	<0.001	-1.5±1.4	**15.0±11.0***	-2.0±1.9	-1.4±1.1	0.3±1.3	**15.6±9.3***	2.1±3.3	0.7±1.9
T_{fall} ($T-T_c$, ms)	24.63	<0.001	2.6±5.6	**31.1±10.0***	-3.6±7.5	-1.9±1.9	-4.7±4.1	**22.8±5.2***	**-13.8±4.1***	-6.9±3.5
W_{sw} ($W-W_c$, Jkg^{-1})	36.56	<0.001	**0.55±0.23***	**-0.62±0.40***	**0.37±0.36***	**0.61±0.36***	**0.36±0.35***	**-1.22±0.20***	0.27±0.50	**0.43±0.28***
W_{Net} ($W-W_c$, Jkg^{-1})	121.74	<0.001	**-1.31±0.19***	**5.26±1.39***	-0.52±0.28	**-1.13±0.44***	-0.41±0.42	**6.05±1.17***	0.48±0.52	-0.23±0.29
E_{sw} ($E/E_{tot,c}$)	2.14	0.030	0.07±0.04	0.05±0.14	0.08±0.10	0.06±0.03	0.03±0.05	0.11±0.12	0.01±0.05	0.02±0.02
E_{tot} ($E/E_{tot,c}$)	19.51	<0.001	0.11±0.13	**0.85±0.37***	0.13±0.12	0.15±0.11	0.06±0.12	**0.84±0.41***	0.12±0.17	0.02±0.12
DF										
L_{T50} ($L/L_{Fpk,c}$)	85.20	<0.001	-0.02±0.02	**0.24±0.05***	0.05±0.02	-0.04±0.04	-0.02±0.02	**0.27±0.08***	0.01±0.02	-0.04±0.02
L_{Fpk} ($L/L_{Fpk,c}$)	35.92	<0.001	**-0.05±0.03***	**0.17±0.05***	0.00±0.02	**-0.05±0.03***	**-0.04±0.03***	**0.17±0.08***	0.01±0.04	**-0.04±0.02***
V_{TD_T50} ($V-V_c$, Ls^{-1})	2.29	0.022	-0.15±1.10	2.03±1.29	0.86±0.55	0.16±1.03	0.59±0.74	1.36±0.98	0.72±0.54	0.75±0.60
V_{T50_Fpk} ($V-V_c$, Ls^{-1})	22.92	<0.001	-0.72±0.28	**-2.33±0.16***	**-1.35±0.38***	-0.59±0.62	-0.59±0.17	**-3.23±0.29***	-0.16±0.67	0.01±0.73
J_{sw} ($J/J_{pk,c}$)	2.91	0.003	0.01±0.01	0.00±0.01	0.00±0.01	0.01±0.01	0.01±0.01	0.01±0.01	0.00±0.01	0.01±0.01
J_{tot} ($J/J_{pk,c}$)	3.44	0.001	0.15±0.05	-0.09±0.17	0.00±0.12	0.01±0.06	-0.03±0.15	**-0.22±0.06***	-0.09±0.02	-0.03±0.01
F_{pk} ($F/F_{pk,c}$)	11.20	<0.001	**0.13±0.02***	**-0.20±0.09***	0.03±0.10	0.04±0.06	-0.02±0.11	**-0.26±0.07***	0.01±0.06	0.01±0.02
T_{rise} ($T-T_c$, ms)	6.46	<0.001	-1.2±1.1	**22.9±13.8***	1.0±5.3	-3.0±2.5	-0.9±2.3	10.0±6.4	1.1±2.8	-0.4±1.0
T_{fall} ($T-T_c$, ms)	18.36	<0.001	3.3±5.0	**24.4±9.5***	-6.0±4.9	0.7±2.0	-2.1±3.5	**29.9±6.4***	**-11.9±4.8***	-5.8±3.3
W_{sw} ($W-W_c$, Jkg^{-1})	14.54	<0.001	0.12±0.26	**-0.85±0.20***	0.14±0.06	0.23±0.17	**0.36±0.33***	**-0.94±0.29***	-0.17±0.22	**0.34±0.20***
W_{Net} ($W-W_c$, Jkg^{-1})	5.66	<0.001	1.08±3.30	9.16±3.84	6.71±1.16	4.15±2.84	2.59±1.29	**13.79±2.85**	3.87±2.35	0.25±5.96
E_{sw} ($E/E_{tot,c}$)	14.63	<0.001	**0.06±0.02***	**-0.05±0.01***	**0.05±0.01***	**0.04±0.02***	**0.07±0.02***	-0.03±0.02	**0.06±0.03***	**0.06±0.02***
E_{tot} ($E/E_{tot,c}$)	3.22	0.001	**0.16±0.05***	0.20±0.26	0.02±0.15	0.07±0.11	**0.17±0.14***	0.13±0.12	0.09±0.07	0.13±0.07

Table 3. Multiple linear regression analysis of the strain, phase and activation factors on total impulse (J_{tot}) and net work (W_{net}). The standardized coefficient (StdCoef) and variance explained by each X factor (r^2).

LG

	J_{tot}		W_{Net}	
	StdCoef	r^2	StdCoef	r^2
L_{T50} ($L/L_{Fpk,c}$)	0.77	**0.60**	0.75	**0.64**
L_{Fpk} ($L/L_{Fpk,c}$)				
V_{T50} ($V\text{-}V_c$, Ls^{-1})	0.30	0.07		
V_{Fpk} ($V\text{-}V_c$, Ls^{-1})			-0.09	0.04
Phase ($_{Fpk\text{-}Lpk}$)				
E_{sw} ($E/E_{tot,c}$)			-0.16	0.01
E_{tot} ($E/E_{tot,c}$)	0.22	0.09	0.18	0.07
Total R^2		0.76		0.76

DF

	J_{tot}		W_{Net}	
	StdCoef	r^2	StdCoef	r^2
L_{T50} ($L/L_{Fpk,c}$)	-0.68	**0.30**	0.26	0.16
L_{Fpk} ($L/L_{Fpk,c}$)				
V_{T50} ($V\text{-}V_c$, Ls^{-1})				
V_{Fpk} ($V\text{-}V_c$, Ls^{-1})			-0.43	**0.31**
Phase ($_{Fpk\text{-}Lpk}$)	0.22	0.01	0.26	0.16
E_{sw} ($E/E_{tot,c}$)	-0.16	0.05		
E_{tot} ($E/E_{tot,c}$)				
Total R^2		0.36		0.63

Figure 1

a


H
L
H
L

b

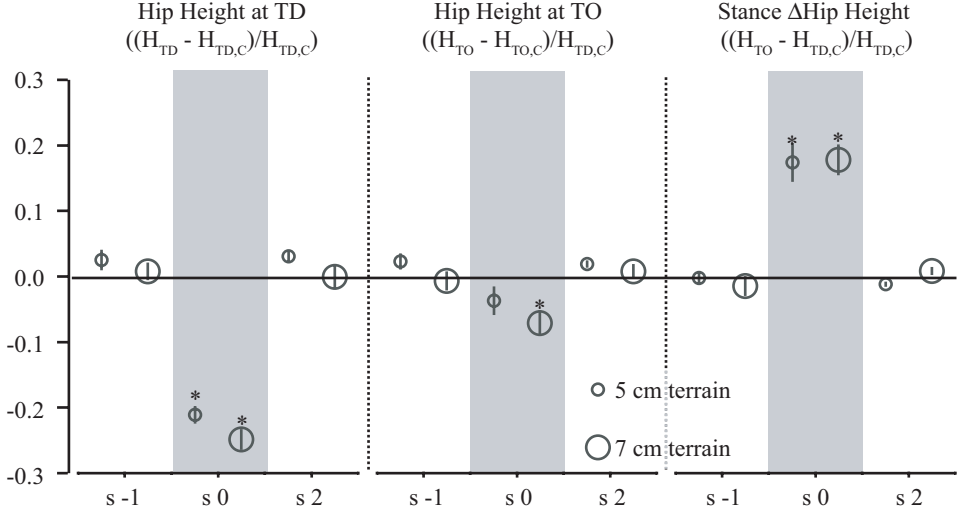
Hip Height at TD
((H_TD - H_TD,C)/H_TD,C)
Hip Height at TO
((H_TO - H_TO,C)/H_TD,C)
Stance ΔHip Height
((H_TO - H_TD,C)/H_TD,C)
0.3
0.2
0.1
0.0
-0.1
-0.2
-0.3
5 cm terrain
7 cm terrain
s -1
s 0
s 2
s -1
s 0
s 2
s -1
s 0
s 2

Figure 2

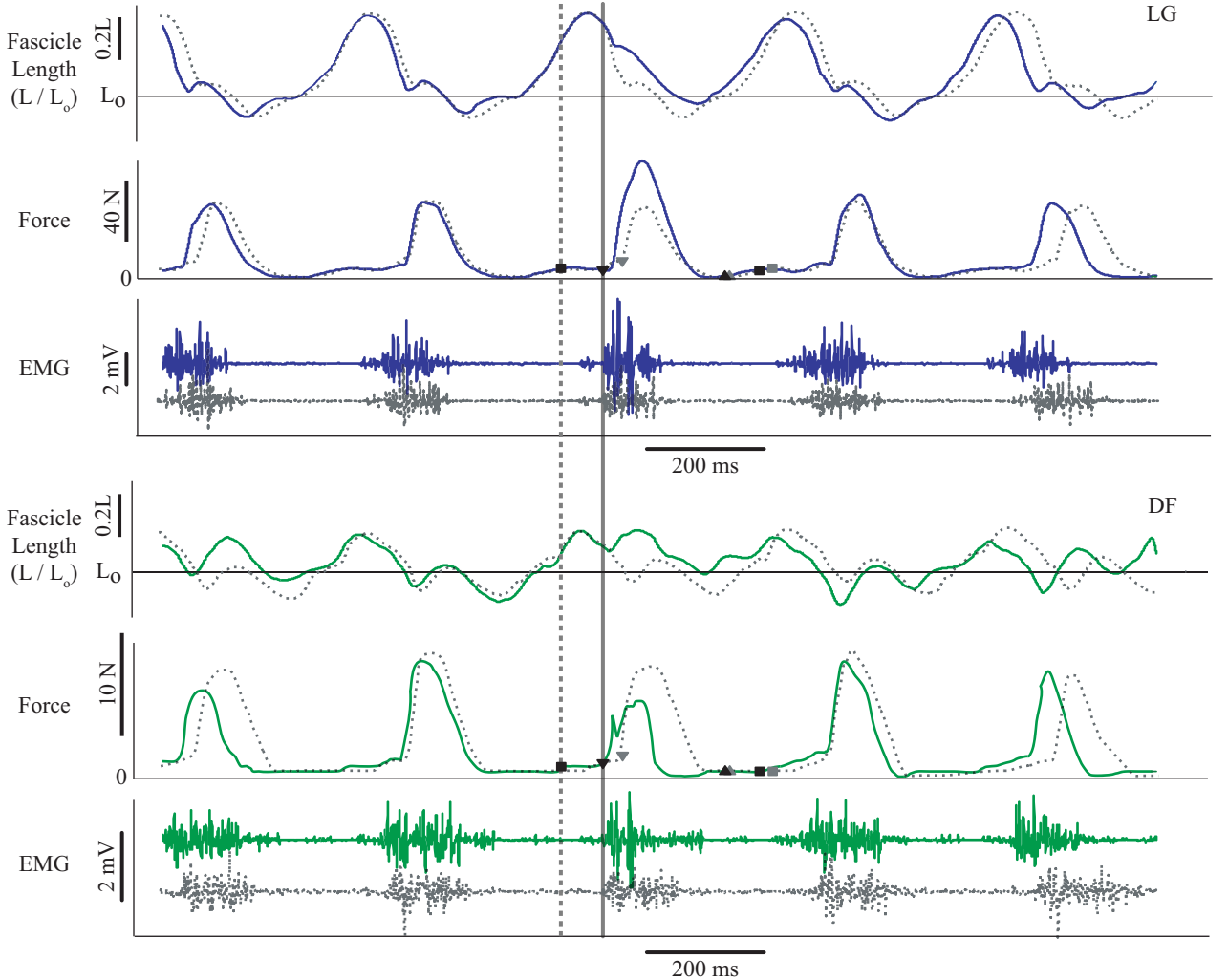
Fascicle Length (L / L$_o$)
0.2L
L$_o$
LG
Force
40 N
0
EMG
2 mV
200 ms
Fascicle Length (L / L$_o$)
0.2L
L$_o$
DF
Force
10 N
0
EMG
2 mV
200 ms

Figure 3

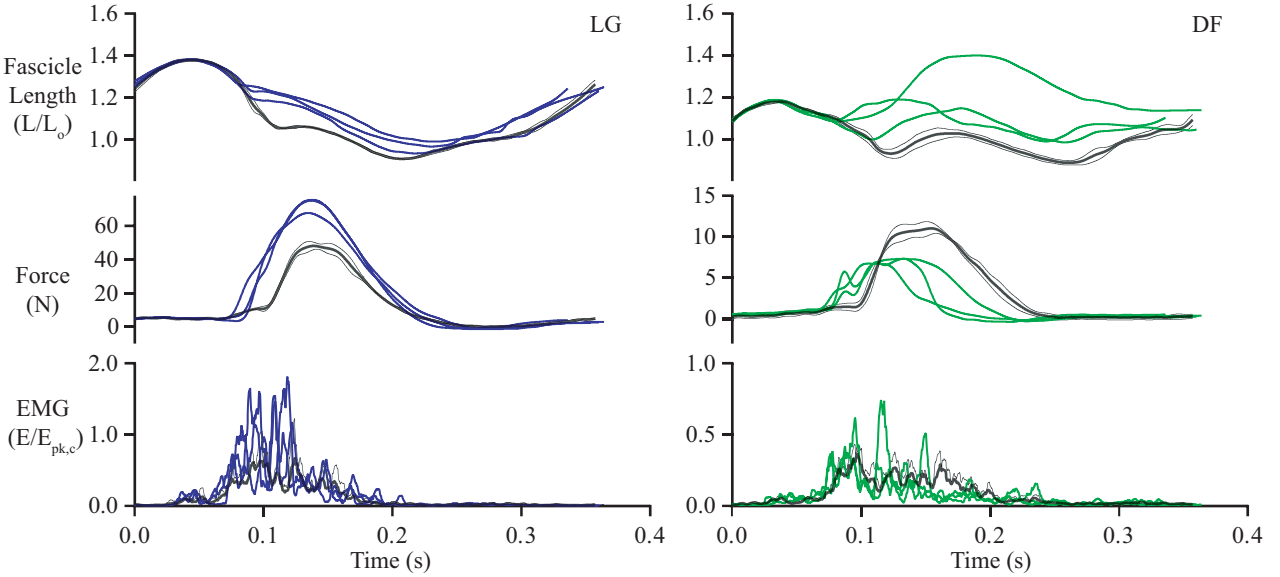
LG
DF
Fascicle Length (L/L_o)
Force (N)
EMG ($E/E_{pk,c}$)
1.6
1.4
1.2
1.0
60
40
20
0
15
10
5
2.0
1.0
0.5
0.0
0.1
0.2
0.3
0.4
Time (s)

Figure 4

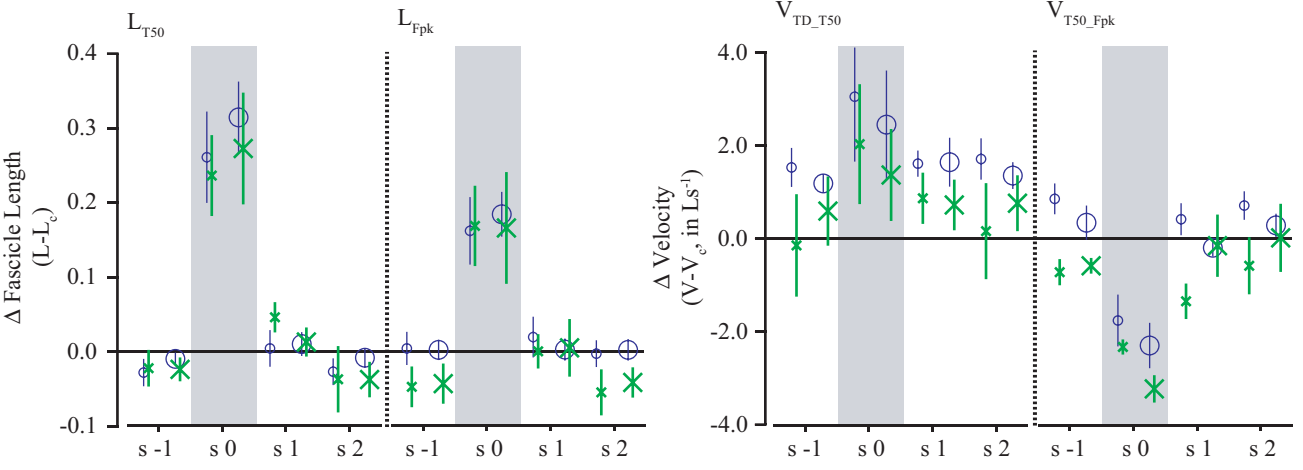
L_T50
L_Fpk
Δ Fascicle Length (L-L_c)
0.4
0.3
0.2
0.1
0.0
-0.1
s -1
s 0
s 1
s 2
V_TD_T50
V_T50_Fpk
Δ Velocity (V-V_c, in Ls^-1)
4.0
2.0
0.0
-2.0
-4.0

Figure 5

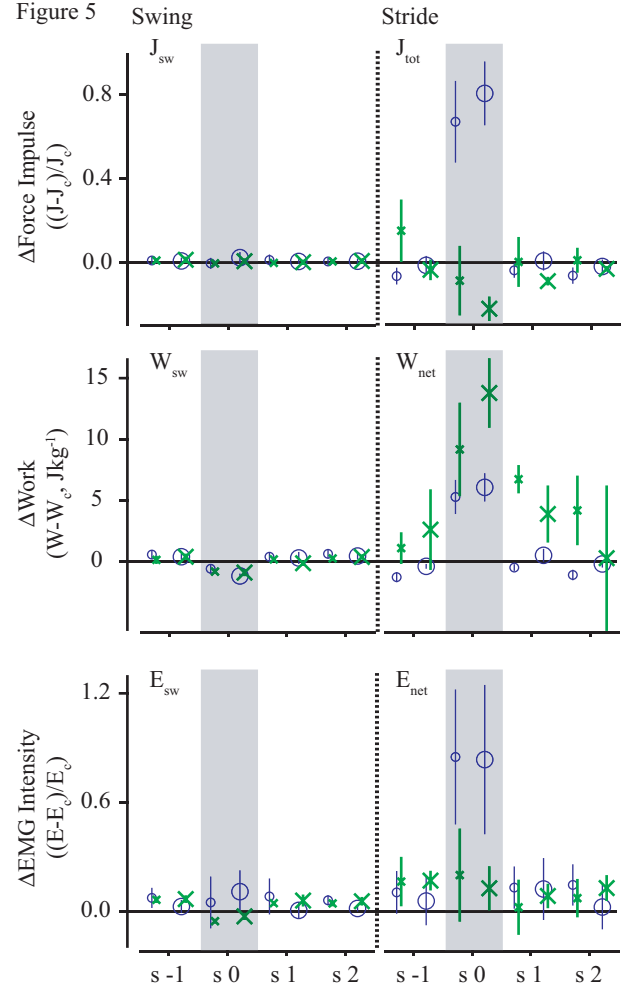
Swing
Stride
J_sw
J_tot
ΔForce Impulse
((J-J_c)/J_c)
0.8
0.4
0.0
W_sw
W_net
ΔWork
(W-W_c, Jkg^-1)
15
10
5
0
E_sw
E_net
ΔEMG Intensity
((E-E_c)/E_c)
1.2
0.6
0.0
s -1
s 0
s 1
s 2
s -1
s 0
s 1
s 2

Figure 6

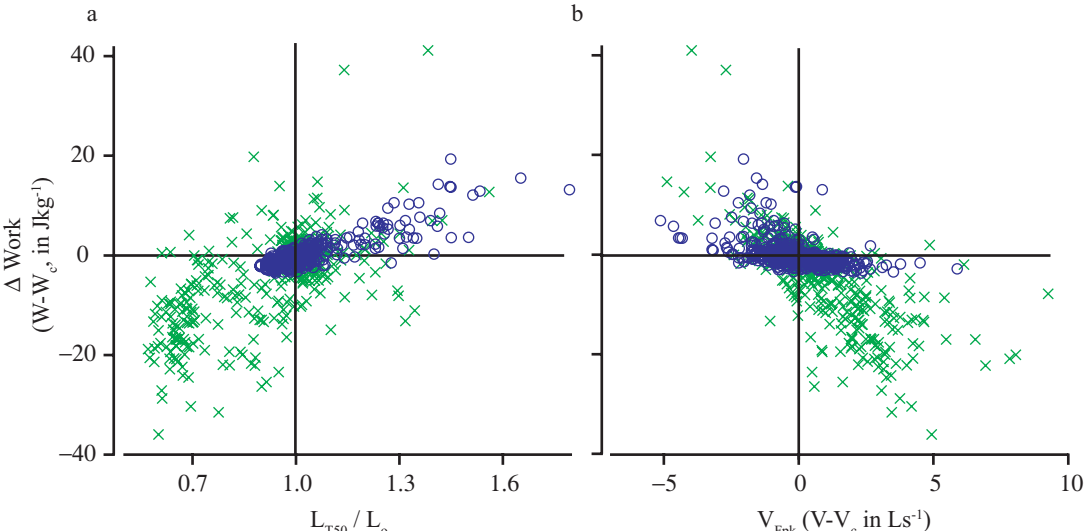
a
b
40
20
0
−20
−40
Δ Work
(W-W$_c$, in Jkg^{-1})
0.7
1.0
1.3
1.6
L$_{T50}$ / L$_o$
−5
0
5
10
V$_{Fpk}$ (V-V$_c$ in Ls^{-1})

Figure 7

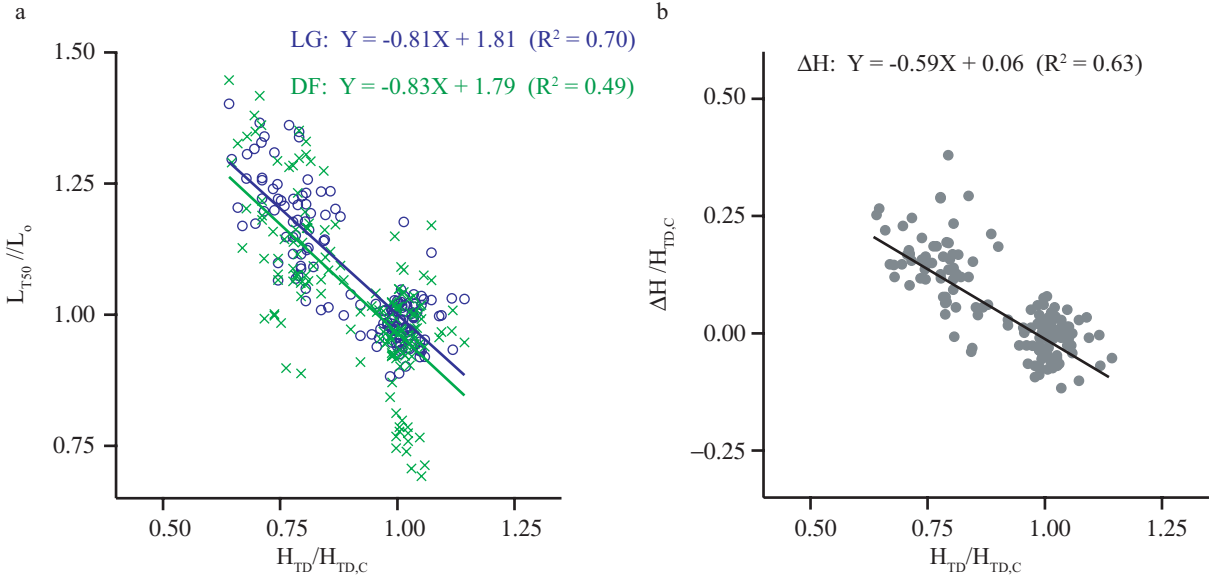
a
LG: Y = -0.81X + 1.81 (R² = 0.70)
DF: Y = -0.83X + 1.79 (R² = 0.49)
1.50
1.25
1.00
0.75
L_T50 /L_o
0.50
0.75
1.00
1.25
H_TD/H_TD,C
b
ΔH: Y = -0.59X + 0.06 (R² = 0.63)
0.50
0.25
0.00
–0.25
ΔH /H_TD,C
0.50
0.75
1.00
1.25
H_TD/H_TD,C

Figure 8

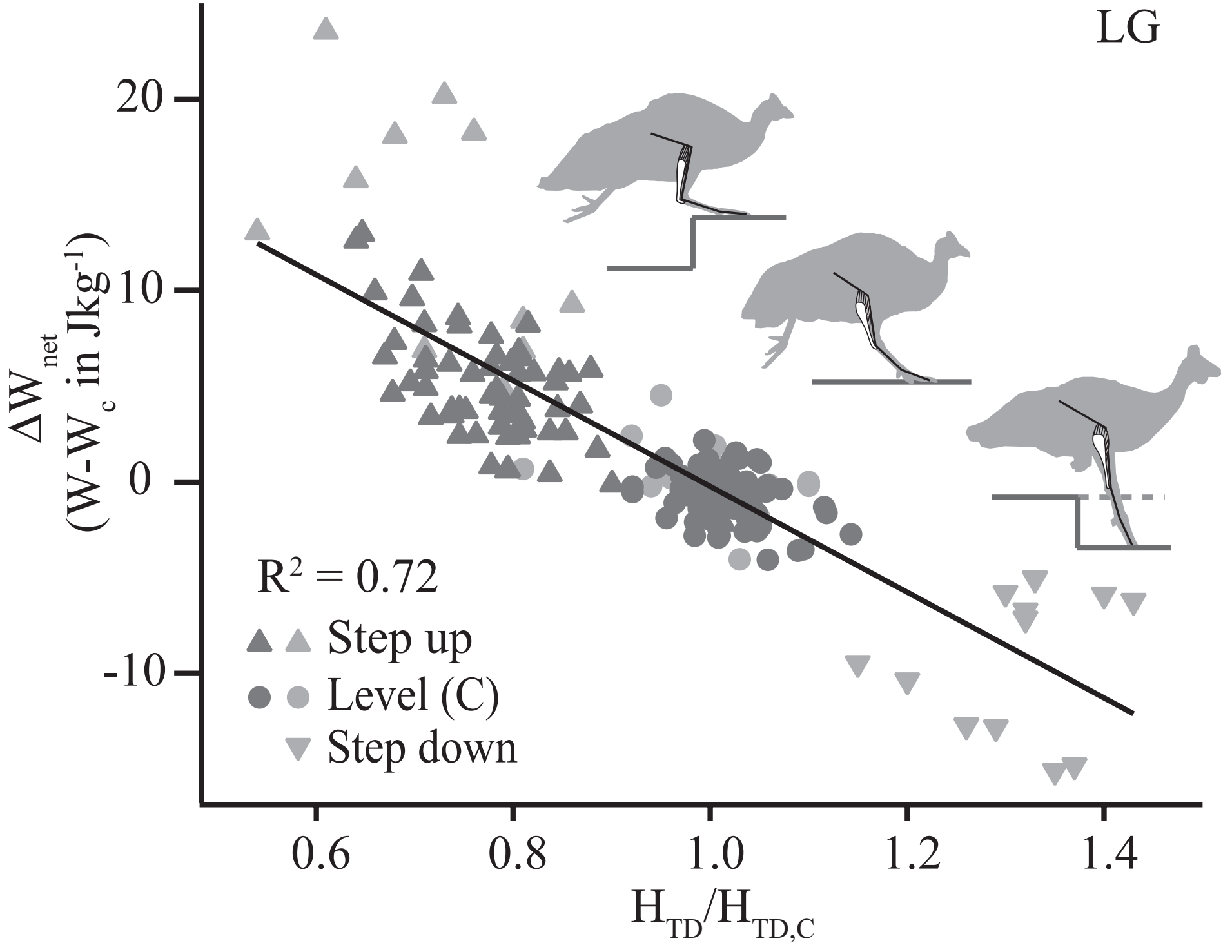
LG
20
10
0
-10
ΔW_{net}
(W-W_c in Jkg^{-1})
$R^2 = 0.72$
Step up
Level (C)
Step down
0.6
0.8
1.0
1.2
1.4
$H_{TD}/H_{TD,C}$